Identifying isomers of peroxy radicals in the gas phase: 1-C3H7O2vs. 2-C3H7O2

Xiaofeng Tang, Xiaoxiao Lin, Gustavo A. Garcia, Jean-Christophe Loison, Zied Gouid, Hassan H. Abdallah, Christa Fittschen, Majdi Hochlaf, Xuejun Gu, Weijun Zhang, et al.

▶ **To cite this version:**

Xiaofeng Tang, Xiaoxiao Lin, Gustavo A. Garcia, Jean-Christophe Loison, Zied Gouid, et al.. Identifying isomers of peroxy radicals in the gas phase: 1-C3H7O2vs. 2-C3H7O2. Chemical Communications, 2020, Chemical Communications, 56 (99), pp.15525-15528. 10.1039/d0cc06516a . hal-03328585

HAL Id: hal-03328585
https://hal.univ-lille.fr/hal-03328585v1

Submitted on 30 Aug 2021

HAL is a multi-disciplinary open access archive for the deposit and dissemination of scientific research documents, whether they are published or not. The documents may come from teaching and research institutions in France or abroad, or from public or private research centers.

L'archive ouverte pluridisciplinaire **HAL**, est destinée au dépôt et à la diffusion de documents scientifiques de niveau recherche, publiés ou non, émanant des établissements d'enseignement et de recherche français ou étrangers, des laboratoires publics ou privés.

Check for updates

View Article Online
View Journal

ChemComm
Chemical Communications

Accepted Manuscript

This article can be cited before page numbers have been issued, to do this please use: X. Tang, X. Lin, G. A. Garcia, J. Loison, Z. Gouid, H. Abdallah, C. Fittschen, M. Hochlaf, X. Gu, W. Zhang and L. Nahon, *Chem. Commun.*, 2020, DOI: 10.1039/D0CC06516A.

This is an Accepted Manuscript, which has been through the Royal Society of Chemistry peer review process and has been accepted for publication.

Accepted Manuscripts are published online shortly after acceptance, before technical editing, formatting and proof reading. Using this free service, authors can make their results available to the community, in citable form, before we publish the edited article. We will replace this Accepted Manuscript with the edited and formatted Advance Article as soon as it is available.

You can find more information about Accepted Manuscripts in the Information for Authors.

Please note that technical editing may introduce minor changes to the text and/or graphics, which may alter content. The journal's standard Terms & Conditions and the Ethical guidelines still apply. In no event shall the Royal Society of Chemistry be held responsible for any errors or omissions in this Accepted Manuscript or any consequences arising from the use of any information it contains.

ROYAL SOCIETY OF CHEMISTRY

rsc.li/chemcomm

Please do not adjust margins

View Article Online
DOI: 10.1039/D0CC06516A

COMMUNICATION

Identifying isomers of peroxy radicals in the gas phase: 1-$C_3H_7O_2$ vs 2-$C_3H_7O_2$†

Received 00th January 20xx,
Accepted 00th January 20xx

DOI: 10.1039/x0xx00000x

Xiaofeng Tang,*[a] Xiaoxiao Lin,[a] Gustavo A. Garcia,[b] Jean-Christophe Loison,[c] Zied Gouid,[d,g] Hassan H. Abdallah,[e] Christa Fittschen,[f] Majdi Hochlaf,*[d] Xuejun Gu,[a] Weijun Zhang[a] and Laurent Nahon*[b]

The two isomers of propylperoxy radical 1-$C_3H_7O_2$ and 2-$C_3H_7O_2$, together with their individual rotamers, are identified and assigned by threshold photoelectron spectroscopy with the aid of high-level theoretical computations, from which their accurate adiabatic ionization energies are derived. This study paves the way to probing elusive peroxy radicals and their isomers in advanced mass spectrometry analysis of combustion and atmospheric reactions.

Peroxy radicals (RO_2) are key reaction intermediates in the low temperature oxidation of organic compounds and play essential roles in combustion and atmospheric chemistry.[1-3] In the atmosphere, they are formed by the reaction of oxygen with alkyl radicals (R), produced from oxidation of organic compounds with oxidizers such as OH, Cl *etc.*, *via* three-body collision reactions,

$$R + O_2 + M \rightarrow RO_2 + M \qquad (1),$$

where M represents a third species removing the excess internal energy of the peroxy radicals. Peroxy radicals can react with various species like NO_x (NO and NO_2), HO_x (OH and HO_2) and other RO_2, as well as performing self and unimolecular reactions, at the core of an abundant chemistry network in the troposphere, controlling the radical cycles and the formation of secondary pollutants such as ozone and secondary organic aerosols.[1] Correspondingly, peroxy radicals have attracted a great deal of attention and are the subject of numerous experimental and theoretical studies.[1-3]

A broad range of methods including absorption spectroscopy,[3] cavity ring-down spectroscopy (CRDS),[4] chemical ionization mass spectrometry (CIMS)[5] and photoionization mass spectrometry (PIMS)[6-8] have been used to analyse peroxy radicals. Among them, PIMS, in particular combined with tunable vacuum ultraviolet (VUV) synchrotron radiation, is seen as a universal analytical method with high sensitivity and selectivity to probe radicals and elucidate their reactions. For example, Fu *et al.* and Meloni *et al.* studied VUV photoionization of alkylperoxy radicals and found that most of their cations are unstable.[8-10] Savee *et al.* observed the hydroperoxyalkyl radical (QOOH), formed via intramolecular H-atom transfer of the peroxy radical in the oxidation of 1,3-cycloheptadiene, by measuring the photoionization efficiency (PIE) curve.[11]

The reaction mechanisms of peroxy radicals often correlate to their structures, which become progressively complex with increasing mass and usually contain several structural isomers (plus their rotamers).[1] The knowledge on peroxy radicals' isomers is very limited and only a few works, mainly from Miller *et al.*, can be found in the literature.[4, 12-14] Miller *et al.* used different precursors to produce the isomers of peroxy radicals and obtained their near infrared CRDS, in which even some rotamers were observed.[4, 13] But, because of restrictions in terms of universality, this spectral region has not been widely used for kinetics.[1] Probing the isomers of peroxy radicals is still challenging, even with the universal and selective VUV synchrotron radiation PIMS due to the instability of their cations,[8-10] limiting mechanistic information on reactions where they might be involved.

Photoelectron photoion coincidence (PEPICO) spectroscopy analyses simultaneously electrons and ions formed by photoionization and can provide spectral fingerprints for very dilute and elusive species in complex reactions by recording photoelectron spectra (PES) for each mass.[15] In addition,

[a] Laboratory of Atmospheric Physico-Chemistry, Anhui Institute of Optics and Fine Mechanics, HFIPS, Chinese Academy of Sciences, Hefei, 230031 Anhui, China. E-mail: tangxf@aiofm.ac.cn
[b] Synchrotron SOLEIL, L'Orme des Merisiers, St. Aubin, BP 48, 91192 Gif sur Yvette, France. E-mail: Laurent.nahon@synchrotron-soleil.fr
[c] Institut des Sciences Moléculaires (ISM), CNRS, Univ. Bordeaux, 351 cours de la Libération, 33400, Talence, France.
[d] Université Gustave Eiffel, COSYS/LISIS, 5 Bd Descartes 77454, Champs sur Marne, France. E-mail: hochlaf@univ-mlv.fr
[e] Department of Chemistry, College of Education, Salahaddin University-Erbil, 44002 Erbil, Iraq.
[f] University Lille, CNRS, UMR 8522, PC2A – Physicochimie des Processus de Combustion et de l'Atmosphère, F-59000 Lille, France.
[g] Laboratoire de caractérisations, applications et modélisations des matériaux. Faculté des Sciences de Tunis, Université Tunis El Manar, 2092-Tunis, Tunisia
X.T., G.G., J.L., C.F., X.G., and L.N. performed the experiments, X.L. and W.Z. calculated potential energy curves, J.L., Z.G., H.A., and M.H. calculated AIEs and Franck-Condon factors, X.T., G.G., M.H., and L.N. wrote the text.
† Electronic Supplementary Information (ESI) available. See DOI: 10.1039/x0xx00000x

Published on 19 November 2020. Downloaded by University of Science and Technology of China on 11/19/2020 2:08:48 PM.

ChemComm Accepted Manuscript

View Article Online DOI: 10.1039/D0CC06546A

Published on 19 November 2020. Downloaded by University of Science and Technology of China on 11/19/2020 2:08:48 PM.

combined with tunable synchrotron radiation as a light source, threshold photoelectron signals can be obtained when the photon energy resonates with the cationic energy level offering much richer and isomer-specific spectral information than PIE.[16, 17] In this work, we present a study on the identification of the two isomers of propylperoxy radical ($C_3H_7O_2$) by using the state-of-the-art method of double imaging PEPICO (i^2PEPICO) spectroscopy[18] available on the VUV beamline DESIRS at SOLEIL French synchrotron radiation source, complemented by accurate theoretical computations on the structure, the vibrational spectra and the energetics of the cationic and neutral species (Fig. 1). A microwave discharge flow tube is employed as chemical reactor to model the low temperature oxidation of propane.[19, 20] The two isomers, 1-$C_3H_7O_2$ and 2-$C_3H_7O_2$, are clearly identified and assigned in the mass-selected threshold photoelectron spectrum (TPES) with the aid of their computed adiabatic ionization energies (AIEs) and Franck-Condon factors. The experimental and theoretical details can be found in the Supplementary Information.

To investigate and decipher the complex chemistry occurring within the flow tube, experiments were performed in two steps. Firstly, propane without oxygen was fed into the flow tube and reacted with fluorine atoms generated by microwave discharge of F_2 to produce the propyl radicals. The two isomers of the propyl radical, 1-C_3H_7 and 2-C_3H_7, are formed through the H-abstraction reactions.

$$F+CH_3CH_2CH_3 \rightarrow HF+CH_3CH_2\dot{C}H_2\ (1\text{-}C_3H_7) \quad (2a)$$

$$F+CH_3CH_2CH_3 \rightarrow HF+CH_3\dot{C}HCH_3\ (2\text{-}C_3H_7) \quad (2b)$$

These reactions have been studied before and the formation ratio of the two isomers was reported at 1-C_3H_7/2-C_3H_7 = 2.3.[21, 22] The photoionization time-of-flight (TOF) mass spectrum integrated in the 7.2–11 eV energy range was measured and is presented in Fig. S1(a). The peak at *m/z* = 43 appears as the

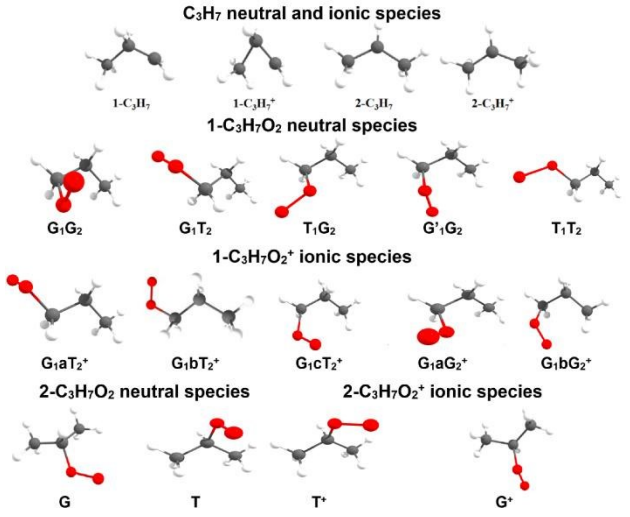

Fig. 1 The stable structures of the isomers of the propyl radical and the propylperoxy radical, together with their cations, obtained at the (R)CCSD(T)-F12/aug-cc-pVDZ level of theory. Their total energies are given in Table S1. For the propylperoxy radical, we used the denomination of Tarczay *et al.*[14] for the isomers and rotamers.

most intense with a narrow width and is assigned to the propyl radical. Its correlated ion image displays a small spot due to the velocity focusing of the i^2PEPICO setup DELICIOUS III,[18, 23] showing the cold character of this nascent species with no kinetic energy release (KER). The *m/z* = 43 ($C_3H_7^+$) cation might be formed from dissociative ionization of the remaining propane precursor in the flow tube, but this possibility is discarded because of the appearance energy of the $C_3H_7^+$ fragment located at 11.59 eV,[24] outside of the aforementioned energy range. In the flow tube the nascent propyl radical self-reacts to produce propene and hexane, which contribute to the *m/z* = 42 and 86 peaks.[25]

The mass-selected photoelectron signal corresponding to the propyl radical was measured in coincidence by scanning the photon energy with a 50 meV step size and is presented in Fig. 2(a). The mass-selected TPES is obtained by integration of the photoelectron signal *I(hν, KE)* along a constant cationic state (diagonal lines), according to the equation below,[26]

$$\mathrm{TPES(hv)} = \int_0^{KE_{max}} I(h\nu + KE, KE)dKE \quad (3).$$

Fig. 2(b) presents the TPES of the propyl radical together with its PIE. In comparison to the smooth variations of the PIE curve, two electronic bands with partially resolved vibrational structures can be observed in the TPES within the 7.3–8.7 eV energy range, providing rich spectral and structural information of the propyl radical. The overall shape of the TPES agrees well with that of the literature TPES by Zichittella *et al.*, in which the vertical ionization energies (VIEs) of 2-C_3H_7 and 1-C_3H_7 locate at ~7.75 and 8.36 eV.[27] In comparison to the HeI PES by Dyke *et al.*,[22] the first band of the TPES is more intense, which might be ascribed to the effect of resonant autoionization in the photon energy scan. The peaks of the two electronic bands in the TPES of Fig. 2(b) locate at 7.72 ± 0.01 and 8.32 ± 0.01 eV and are thus assigned to the ionization of the 2-C_3H_7 and 1-C_3H_7 isomers, respectively. It can be noted that the integrated area ratio of the PIE of 1-C_3H_7 and 2-C_3H_7 is different to the value of 2.3 previously determined,[21] suggesting that these two radicals have different self-reactivity and/or ionization cross sections.

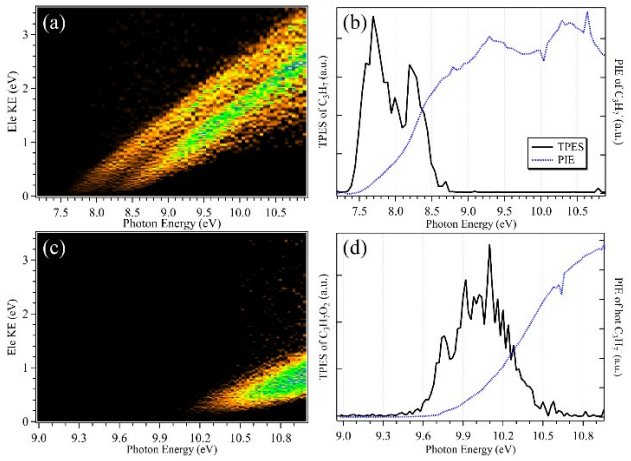

Fig. 2 Mass-selected photoelectron kinetic energy matrices and TPES corresponding to the *m/z* = 43 cations acquired (a, b) without and (c, d) after adding oxygen into the flow tube, together with the PIE curves.

ChemComm Accepted Manuscript

This journal is © The Royal Society of Chemistry 20xx

View Article Online
DOI: 10.1039/D0CC06516A

Published on 19 November 2020. Downloaded by University of Science and Technology of China on 11/19/2020 2:08:48 PM.

Subsequent addition of oxygen into the flow tube leads to several product channels by reactions with propyl radicals that have been proposed and observed, as listed below.[28]

$C_3H_7 + O_2 \rightarrow C_3H_6 + HO_2$ (4a)

$C_3H_7 + O_2 \rightarrow C_3H_6O + OH$ (4b)

$CH_3CH_2\dot{C}H_2+O_2+M \rightarrow CH_3CH_2CH_2O\dot{O}$ (1-$C_3H_7O_2$)+M (4c)

$CH_3\dot{C}HCH_3+O_2+M \rightarrow CH_3CH(O\dot{O})CH_3$ (2-$C_3H_7O_2$)+M (4d)

Note that the propylperoxy radical should be produced as two isomers, 1-$C_3H_7O_2$ and 2-$C_3H_7O_2$, together with their individual rotamers, *i.e.* the G_1G_2, G_1T_2, T_1G_2, T_1T_2 and $G_1'G_2$ of 1-$C_3H_7O_2$, and the G and T of 2-$C_3H_7O_2$ (cf. Fig. 1).[13, 14]

Fig. S1(b) presents the mass spectrum integrated in the 9–11 eV energy range after addition of oxygen into the flow tube. The peaks at *m/z* 42 and 58 are assigned as the products C_3H_6 (Eq. 4a) and C_3H_6O (Eq. 4b). Previous studies have demonstrated that the propylperoxy cation $C_3H_7O_2^+$ is unstable and dissociates into fragments $C_3H_7^+$ and O_2,[8, 9, 28] and thus no signal is observed at *m/z* 75. The other minor peaks are ascribed to the products of secondary reactions inside the flow tube.[28]

Our theoretical calculations indicate that the ground state of the $C_3H_7O_2^+$ is of X^3A'' nature with large geometrical changes between the neutral and cationic ground states (Fig. S2). These result in weak and undetected transitions to populate the $C_3H_7O_2^+$ (X^3A'') within the present energy range. Conversely, the a^1A' first excited states of the cations are calculated to be bound with C-O bond lengths at 1.46 and 1.56 Å, close to those of the neutral X^2A'' ground state, and should be predominantly populated by the photoionization process. The potential energy curve of the a^1A' state crosses the X^3A''state at ~1.8(1.9) Å and their interaction, e.g. via spin-orbit coupling, can induce the predissociation of the $C_3H_7O_2^+$(a^1A') ions into the $C_3H_7^+$ and O_2 fragments, which explains why the $C_3H_7O_2^+$ cations are unstable and why only the $C_3H_7^+$ fragment ions can be observed in the mass spectrum.[8, 9, 28] The pre-dissociation is fast and a large ratio of the available energy upon dissociation (~1 eV) is released into the kinetic energies of the fragments. Indeed, the derived KER of $C_3H_7^+$ displayed in Fig. S1(b) shows a broad curve with attainable ion kinetic energies up to 0.8 eV when oxygen is added, in stark contrast with the narrow distribution in Fig. S1(a) obtained without oxygen.

Fig. 2(c) and 2(d) show the mass-selected photoelectron kinetic energy matrix and the TPES in the 9–11 eV energy range (with a 20 meV step size) corresponding to the $C_3H_7^+$ fragment ion in Fig. S1(b), *i.e.* in oxygenated conditions. In Fig. 2(b), corresponding to the TPES of the propyl radical, no electron signals are observed in the 9–11 eV range. Thus the broad band in the 9.4-10.7 eV range, superimposed with fine vibrational structures in the TPES of Fig. 2(d), originates solely from the propylperoxy radical, *i.e.* from its fragmentation into a hot $C_3H_7^+$ ion. Moreover, in the photoelectron matrix and in the TPES of the propylperoxy radical no electronic signals can be observed at ~ 9.0 eV, close to the calculated AIEs (8.68 and 8.88 eV) of the X^3A'' ground state, indicating that the X^3A'' state is not populated in the photoionization, consistent with the above theoretical calculations. The AIEs of the a^1A' electronic state of 2-$C_3H_7O_2^+$ and 1-$C_3H_7O_2^+$ are calculated at 9.74 and 9.88 eV (most intense transition from G_1T_2), as listed in Table 1, in very good agreement with the first two peaks of the TPES measured at 9.759 ± 0.005 and 9.919 ± 0.005 eV in Fig. 2(d). The error bars mainly include the uncertainty in the photon energy calibration, the influence of the scanning step size and the signal-to-noise ratio of the TPES[29]. Worth noting the good performance of the less computationally demanding PBE0/aug-cc-pVDZ (optg)//(R)CCSD(T)-F12/aug-cc-pVTZ (SP) + ZPVE (PBE0/aug-cc-pVDZ) composite scheme with respect to the costly (R)CCSD(T)-F12/aug-cc-pVTZ (optg) +ZPVE (PBE0/aug-cc-pVDZ approach.

In order to assign the TPES, the Franck-Condon factors for the ionization transitions of the two isomers 1-$C_3H_7O_2$ and 2-$C_3H_7O_2$, from their neutral X^2A'' ground state to the cationic a^1A' excited state, have been calculated at the M062X/aug-cc-pVTZ level. Only the G_1G_2, G_1T_2, $G_1'G_2$ and G rotamers show favourable Franck-Condon factors. The calculated PES of these rotamers are obtained from the Franck-Condon factors and presented in Fig. 3. The relative ratio between the 1- and 2-

Table 1. Calculated adiabatic ionisation energies (AIEs, eV) of the propylperoxy radicals' isomers and rotamers. See Table S1 for details. For other photoionization transitions, see Table S2.

	Photoionization transition [a]	AIEs [b]	AIEs [c]
1-$C_3H_7O_2$	$G_1T_2 \rightarrow G_1aT_2^+$	9.90	9.88
	$G_1G_2 \rightarrow G_1aG_2^+$	9.94	9.90
	$G_1'G_2 \rightarrow G_1bG_2^+$	- -	9.80
	TPES		9.919 ± 0.005
2-$C_3H_7O_2$	$G \rightarrow G^+$	9.76	9.74
	TPES		9.759 ± 0.005

[a] To populate the lowest singlet cationic state.
[b] Using the PBE0/aug-cc-pVDZ (optg)//(R)CCSD(T)-F12/aug-cc-pVTZ (SP) + ZPVE (PBE0/aug-cc-pVDZ) composite scheme.
[c] Using the (R)CCSD(T)-F12/aug-cc-pVTZ (optg) +ZPVE (PBE0/aug-cc-pVDZ or M06-2X/AVTZ) level composite scheme.

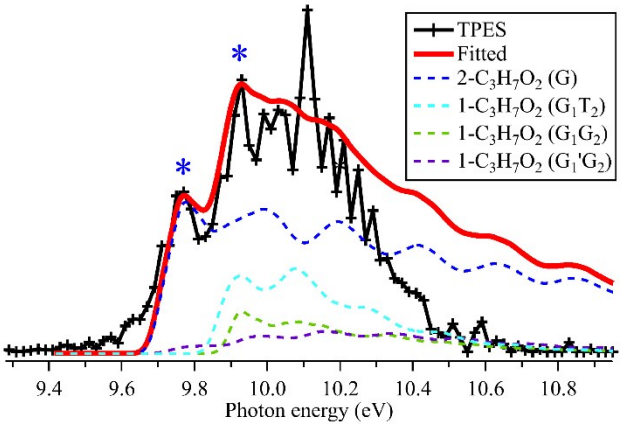

Fig. 3 TPES of the propylperoxy radical and the fitted result with the calculated PES of the G_1G_2, G_1T_2, $G_1'G_2$, and G rotamers, where the vibrational origin (0-0) bands of the a^1A' state of 1-$C_3H_7O_2^+$ and 2-$C_3H_7O_2^+$ are marked with stars. The simulated PES have been convolved with a 35 meV Gaussian to match the width of the observed bands, and shifted by -19 meV (2-$C_3H_7O_2$) and -39 meV (1- $C_3H_7O_2$).

ChemComm Accepted Manuscript

Published on 19 November 2020. Downloaded by University of Science and Technology of China on 11/19/2020 2:08:48 PM.

$C_3H_7O_2$ isomers has been adjusted to best match the experimental TPES, whereas the rotamer relative contribution to each isomer is kept constant to that given by the FC calculations. The agreement between the fitted and the experimental data is satisfactory, as shown in Fig. 3, although some differences can be observed at higher photon energy. One of the reasons for this discrepancy could lie in the fact that the TPES of the propylperoxy radical is directly acquired from the electron signal of the $C_3H_7^+$ fragment and so its intensity should be somewhat affected by the vibrationally energy-dependent dissociation dynamics of $C_3H_7O_2^+$, such as the spin-orbit coupling predissociation of the a^1A' state by the X^3A'' state, which deserves to be theoretically studied in the future. Moreover, autoionization resonances could also influence the shape of the TPES. Nevertheless, the comparison between the fitted and experimental TPES spectra confirm that the first two peaks correspond to the a^1A' state of 2-$C_3H_7O_2^+$ (AIE = 9.759 ± 0.005 eV) and that of 1-$C_3H_7O_2^+$ (AIE = 9.919 ± 0.005 eV).

In conclusion, we have identified the isomers of the propylperoxy radical, generated in the microwave discharge flow tube initiated with fluorine atoms in the C_3H_8/O_2/He mixture, through their photoelectron spectroscopic characterization by using the state-of-the-art method of i^2PEPICO complemented by accurate theoretical computations on the structure and the spectra of the neutrals and the cations. Calculated potential energy curves show that upon photoionization the propylperoxy cation $C_3H_7O_2^+$ is not stable and completely dissociates into the $C_3H_7^+$ and O_2 fragments, making its experimental analysis challenging. Thus two kinds of $C_3H_7^+$ cation, from ionization of the propyl radical and from dissociative ionization of the propylperoxy radical, are observed with different ion kinetic energies, and have been separated spectrally in coincidence. The isomers of the propylperoxy radical, 1-$C_3H_7O_2$ and 2-$C_3H_7O_2$, together with their individual rotamers, are clearly identified and unambiguously assigned in the mass-selected TPES with the aid of theoretical calculations. In addition, the AIEs of the isomers 1-$C_3H_7O_2$ and 2-$C_3H_7O_2$ are determined for the first time, with an accuracy of 0.005 eV, and are in very good agreement with the present high level theoretical results.

This work exemplifies the capabilities of i^2PEPICO complemented by advanced computations, as a powerful method able to provide new insights into on-line analysis of complex gas-phase chemistry reactions, such as combustion and atmospheric oxidation, through isomer identification of elusive radical intermediates such as the propylperoxy radical presented here. Finally, the coincident ion kinetic energy distributions offer further analytical advantages to distinguish fragment (dissociative ionization) from parent (direct ionization) ions, as demonstrated here and recently applied to the quantification of ketohydroperoxides in low temperature combustion of alkanes[30].

This work was supported by the National Natural Science Foundation of China (21773249, 91961123, 91544228), the International Partnership Program of Chinese Academy of Sciences (116134KYSB20170048), the French Agence Nationale de la Recherche (ANR-12-BS08-0020-02) and SOLEIL (20150802).

Conflicts of interest

View Article Online
DOI: 10.1039/D0CC06516A

There are no conflicts to declare.

Notes and references

1 J. J. Orlando and G. S. Tyndall, *Chem. Soc. Rev.*, 2012, **41**, 6294.
2 C. K. Westbrook, *P. Combust. Inst.*, 2000, **28**, 1563.
3 G. S. Tyndall, R. A. Cox, C. Granier, R. Lesclaux, G. K. Moortgat, *et al.*, *J. Geophys. Res.-Atmos.*, 2001, **106**, 12157.
4 E. N. Sharp, P. Rupper and T. A. Miller, *Phys. Chem. Chem. Phys.*, 2008, **10**, 3955.
5 T. Berndt, W. Scholz, B. Mentler, L. Fischer, H. Herrmann, *et al.*, *Angew. Chem. Int. Ed.*, 2018, **57**, 3820.
6 D. L. Osborn, P. Zou, H. Johnsen, C. C. Hayden, C. A. Taatjes, *et al.*, *Rev. Sci. Instrum.*, 2008, **79**, 104103.
7 Z. Wen, X. Tang, C. Wang, C. Fittschen, T. Wang, *et al.*, *Int. J. Chem. Kinet.*, 2019, **51**, 178.
8 H. B. Fu, Y. J. Hu and E. R. Bernstein, *J. Chem. Phys.*, 2006, **125**, 014310.
9 G. Meloni, P. Zou, S. J. Klippenstein, M. Ahmed, S. R. Leone, *et al.*, *J. Am. Chem. Soc.*, 2006, **128**, 13559.
10 G. Meloni, T. M. Selby, F. Goulay, S. R. Leone, D. L. Osborn, *et al.*, *J. Am. Chem. Soc.*, 2007, **129**, 14019.
11 J. D. Savee, E. Papajak, B. Rotavera, H. Huang, A. J. Eskola, *et al.*, *Science*, 2015, **347**, 643.
12 S. J. Zalyubovsky, B. G. Glover, T. A. Miller, C. Hayes, J. K. Merle, *et al.*, *J. Phys. Chem. A*, 2005, **109**, 1308.
13 G. M. P. Just, P. Rupper, T. A. Miller and W. L. Meerts, *Phys. Chem. Chem. Phys.*, 2010, **12**, 4773.
14 G. Tarczay, S. J. Zalyubovsky and T. A. Miller, *Chem. Phys. Lett.*, 2005, **406**, 81.
15 T. Baer and R. P. Tuckett, *Phys. Chem. Chem. Phys.*, 2017, **19**, 9698.
16 E. Reusch, F. Holzmeier, P. Constantinidis, P. Hemberger and I. Fischer, *Angew. Chem. Int. Ed.*, 2017, **56**, 8000.
17 J. Bourgalais, Z. Gouid, O. Herbinet, G. A. Garcia, P. Arnoux, *et al.*, *Phys. Chem. Chem. Phys.*, 2020, **22**, 1222.
18 G. A. Garcia, B. K. C. de Miranda, M. Tia, S. Daly and L. Nahon, *Rev. Sci. Instrum.*, 2013, **84**, 053112.
19 G. A. Garcia, X. Tang, J.-F. Gil, L. Nahon, M. Ward, *et al.*, *J. Chem. Phys.*, 2015, **142**, 164201.
20 X. Tang, X. Gu, X. Lin, W. Zhang, G. A. Garcia, *et al.*, *J. Chem. Phys.*, 2020, **152**, 104301.
21 R. Foon and G. P. Reid, *Trans. Faraday Soc.*, 1971, **67**, 3513.
22 J. Dyke, A. Ellis, N. Jonathan and A. Morris, *J. Chem. Soc., Faraday Trans. II*, 1985, **81**, 1573.
23 X. Tang, G. A. Garcia, J. F. Gil and L. Nahon, *Rev. Sci. Instrum.*, 2015, **86**, 123108.
24 W. A. Chupka and J. Berkowitz, *J. Chem. Phys.*, 1967, **47**, 2921.
25 H. Adachi and N. Basco, *Int. J. Chem. Kinet.*, 1981, **13**, 367.
26 J. C. Poully, J. P. Schermann, N. Nieuwjaer, F. Lecomte, G. Gregoire, *et al.*, *Phys. Chem. Chem. Phys.*, 2010, **12**, 3566.
27 G. Zichittella, P. Hemberger, F. Holzmeier, A. Bodi and J. Perez-Ramirez, *J. Phys. Chem. Lett.*, 2020, **11**, 856.
28 O. Welz, M. P. Burke, I. O. Antonov, C. F. Goldsmith, J. D. Savee, *et al.*, *J. Phys. Chem. A*, 2015, **119**, 7116.
29 J. W. Brault, *Mikrochimica Acta*, 1987, **3**, 215.
30 F. Battin-Leclerc, J. Bourgalais, Z. Gouid, O. Herbinet, G. Garcia, *et al.*, *P. Combust. Inst.*, 2020, DOI: 10.1016/j.proci.2020.06.159.

ChemComm Accepted Manuscript

 This journal is © The Royal Society of Chemistry 20xx

Electronic Supplementary Material (ESI) for ChemComm.
This journal is © The Royal Society of Chemistry 2020

Supplementary Information

Identifying isomers of peroxy radicals in the gas phase: 1-$C_3H_7O_2$ vs 2-$C_3H_7O_2$

Xiaofeng Tang,*[a] Xiaoxiao Lin,[a] Gustavo A. Garcia,[b] Jean-Christophe Loison,[c] Zied Gouid,[d,g] Hassan H. Abdallah,[e] Christa Fittschen,[f] Majdi Hochlaf,*[d] Xuejun Gu,[a] Weijun Zhang[a] and Laurent Nahon*[c]

Experimental and Theoretical Details

Experiments were carried out with the i^{2}PEPICO spectrometer, DELICIOUS III, on the undulator-based VUV beamline DESIRS at synchrotron SOLEIL, France.[1, 2] Synchrotron radiation photons were dispersed by a 6.65 m normal incidence monochromator with a 200 l.mm^{-1} grating and the photon energy resolution was set at ~3 meV. A gas filter filled with Kr was utilized to suppress high harmonics emitted from the undulator that could be transmitted by the grating's high-orders. A flow tube was employed as chemical reactor to model and study the low temperature oxidation of propane, in which fluorine atoms produced from diluted F_2 gas in helium (5%, 15 sccm) with a microwave discharge generator (Sairem, 2.45 GHz) were used to initiate reactions.[3, 4] Reactants like propane and oxygen, together with helium carrier gas, were added and the total gas flow rate was fixed at 1600 sccm with a 2 mbar pressure inside the flow tube. The gas mixture was sampled through two skimmers (1 mm diameter) and crossed the photon beam at the center of DELICIOUS III,[2, 5] where photoelectrons and photoions produced by photoionization were extracted and accelerated in opposite directions towards an electron velocity map imaging (VMI) device and a modified Wiley-McLaren ion momentum imager analyzer. The ion 3D velocity distribution is derived from the TOF and the arrival position. The photoelectron images were filtered by ion mass and velocity, and subsequently Abel inverted [6] to obtain the electron kinetic energy distribution and TPES.

Computations consisted of the determinations of the structures of the neutral and ionic species of $C_3H_7O_2$ sum formula and of the corresponding the adiabatic ionization energies (AIEs), potential energy curves and Franck-Condon factors. Concretely, the geometry optimizations, without constraints (in the C_1 point group), of the stable forms of the neutral and the cationic species of $C_3H_7O_2$, followed by (an)harmonic frequency computations to ensure the minimal nature of the optimized structures, were done at the PBE0/aug-cc-pVDZ level as implemented in the GAUSSIAN 09 program package.[7] We also performed full optimization of the structures at the explicitly correlated coupled cluster single-double and perturbative triple excitations approach, (R)CCSD(T)-F12 in conjunction with the aug-cc-pVTZ basis set[8] as implemented in MOLPRO 2015 [9]. Afterwards, we derived the AIEs of the $C_3H_7O_2$ isomers using either the PBE0/aug-cc-pVDZ(opt)//(R)CCSD(T)-F12/aug-cc-pVDZ(SP)[10, 11] composite scheme or at the (R)CCSD(T)-F12/aug-cc-pVDZ level (denoted (R)CCSD(T)-F12 /aug-cc-pVDZ (opt)). Within the composite scheme, single point (SP) calculations using the (R)CCSD(T)-F12/aug-cc-pVTZ approach[8], are done at the PBE0/aug-cc-pVDZ optimized geometries. The full set of results are listed in Table S1 and Table S2. The composite scheme PBE0/aug-cc-pVDZ(opt)//(R)CCSD(T)-F12/aug-cc-pVDZ(SP)[10, 11] is viewed to allow derivation of accurate energetics up to ± 0.02 eV (including AIEs) as established for a wide range of small and medium sized compounds, also including “unstable” radicals and ions.[12, 13]

The Franck-Condon factors for the ionization transitions of $C_3H_7O_2$, as well as for the geometry and harmonic frequency calculations required as input parameters, were calculated at the M062X/aug-cc-pVTZ level of theory using the time-independent adiabatic Hessian Franck-Condon model in the GAUSSIAN program.[7] The data are given in Fig. 3.

The potential energy curves of the low-lying electronic states of the neutral and the cationic $C_3H_7O_2$ along the C-O coordinate (Fig. S2) were calculated at the QCISD(T)/cc-pVTZ level of theory in the GAUSSIAN program.[7]

Results

Table S1. Computed equilibrium structures of the isomers and rotamers of the propylperoxy radical, together with their cations, obtained at the PBE0/aug-cc-pVDZ and (R)CCSD(T)-F12/aug-cc-pVDZ levels of theory. We give also their PBE0/aug-cc-pVDZ total energies (in Hartree) and zero point vibrational energies ZPVE (in eV) and (R)CCSD-F12(T)/aug-cc-pVDZ computations total energies (in Hartree). For the propylperoxy radical, we used the denomination of Tarczay *et al.*[14] for the isomers and rotamers. For the neutrals we computed the lowest doublet state and for the cation we computed the lowest singlet state.

Method/basis set	**1-$C_3H_7O_2$ neutral species**				
	G_1G_2	**G_1T_2**	**T_1G_2**	**G'_1G_2**	**T_1T_2**
PBE0/aug-cc-pVDZ (opt) [a]	-268.58289042	-268.58282837	-268.58245543	-268.58207934	-268.5823823
ZPVE /PBE0/aug-cc-pVDZ (opt) [a]	2.73	2.73	2.72	2.72 2.76[c]	2.72
RCCSD(T)-F12 /aug-cc-pVDZ (SP) [b]	-268.47907369	-268.47882282	-268.47848217	-268.47828718	-268.47827678
RCCSD(T)-F12 /aug-cc-pVDZ (opt) [a]	-268.47941948	-268.47915014	-268.47884503	-268.47862173	-268.47862221
Relative energy (cm^{-1}) [a], [d]	0	59	126	175	175
	1-$C_3H_7O_2^+$ ionic species				
	$G_1aT_2^+$	**$G_1bT_2^+$**	**$G_1cT_2^+$**	**$G_1aG_2^+$**	**$G_1bG_2^+$**
PBE0/aug-cc-pVDZ (opt) [a]	-268.2124092	-268.212061812	-268.4534305[c]	-268.21096674	-268.4571536[c]
ZPVE /PBE0/aug-cc-pVDZ (opt) [a]	2.70	2.64	2.72[c]	2.69	2.72[c]
CCSD(T)-F12 /aug-cc-pVDZ (SP) [b]	-268.11341454	-268.11302719	-	-268.11201897	-

CCSD(T)-F12 /aug-cc-pVDZ (opt) [a]	-268.11496856	-268.11479234	-268.11438085	-268.11395345	-268.11702749
	2-$C_3H_7O_2$ neutral species		**2-$C_3H_7O_2^+$ ionic species**		
	G	**T**	**T^+**	**G^+**	
PBE0/aug-cc-pVDZ (opt) [a]	-268.5886508	-268.58801268	-268.2242517	-268.2213351	
ZPVE /PBE0/aug-cc-pVDZ (opt) [a]	2.70	2.71	2.67	2.67	
(R)CCSD(T)-F12 /aug-cc-pVDZ (SP) [b]	-268.48532326	-268.48469911	-268.12587128	-268.12535720	
(R)CCSD(T)-F12 /aug-cc-pVDZ (opt) [a]	-268.48567130	-268.48502450	-268.12745737	-268.12652401	
Relative energy (cm^{-1}) [a], [d]	0	142			

[a] Full optimisation.

[b] Single point computations at the PBE0/aug-cc-pVDZ optimized geometry.

[c] Optimised at the M06-2X/aug-cc-pTVZ level of theory.

[c] Relative energy to the most stable rotamer.

Table S2. Calculated adiabatic ionisation energies (AIEs, eV) of the propylperoxy radicals' isomers and rotamers. See Table S1 for details.

Photoionization transition [a]	AIE [b]	AIE [c]
1-$C_3H_7O_2$		
$G_1G_2 \rightarrow G_1aT_2^+$	9.92	9.88
$G_1T_2 \rightarrow G_1aT_2^+$	9.90	9.88
$T_1G_2 \rightarrow G_1aT_2^+$	9.91	9.88
$G'_1G_2 \rightarrow G_1aT_2^+$	9.92	9.87
$T_1T_2 \rightarrow G_1aT_2^+$	9.90	9.87
$G_1G_2 \rightarrow G_1aG_2^+$	9.94	9.90
$G_1T_2 \rightarrow G_1aG_2^+$	9.94	9.90
$T_1G_2 \rightarrow G_1aG_2^+$	9.94	9.90
$G'_1G_2 \rightarrow G_1aG_2^+$	9.93	9.89
$T_1T_2 \rightarrow G_1aG_2^+$	9.93	9.89
$G_1T_2 \rightarrow G_1bT_2^+$	9.86	9.82
2-$C_3H_7O_2$		
$G \rightarrow G^+$	9.76	9.74
$G \rightarrow T^+$	9.75	9.71
$T \rightarrow G^+$	9.73	9.71
$T \rightarrow T^+$	9.72	9.69

[a] To populate the lowest singlet cationic state a^1A'.

[b] Using the PBE0/aug-cc-pVDZ (optg)//(R)CCSD(T)-F12/aug-cc-pVTZ+ZPVE (SP) composite scheme.

[c] Using the (R)CCSD(T)-F12/aug-cc-pVTZ+ZPVE level after full optimisation.

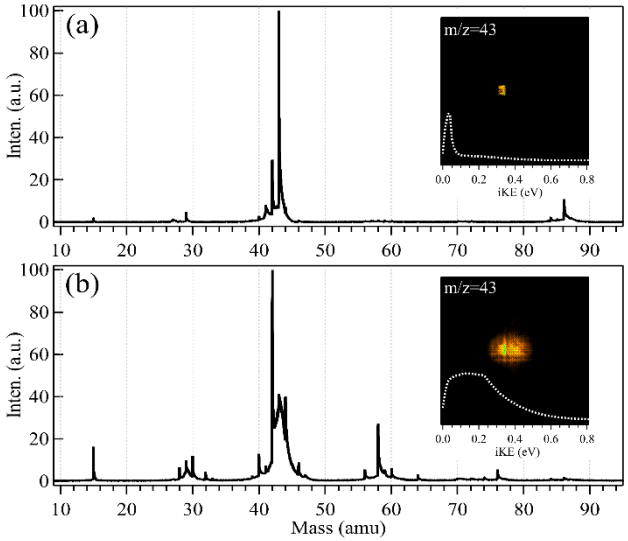

Fig. S1 Photoionization TOF mass spectra and the *m/z* 43 ion images acquired (a) without (integrated in the 7.2-11 eV range) and (b) with (integrated in the 9-11 eV range) addition of oxygen into the flow tube, together with its kinetic energy distributions (iKE, white dashed lines).

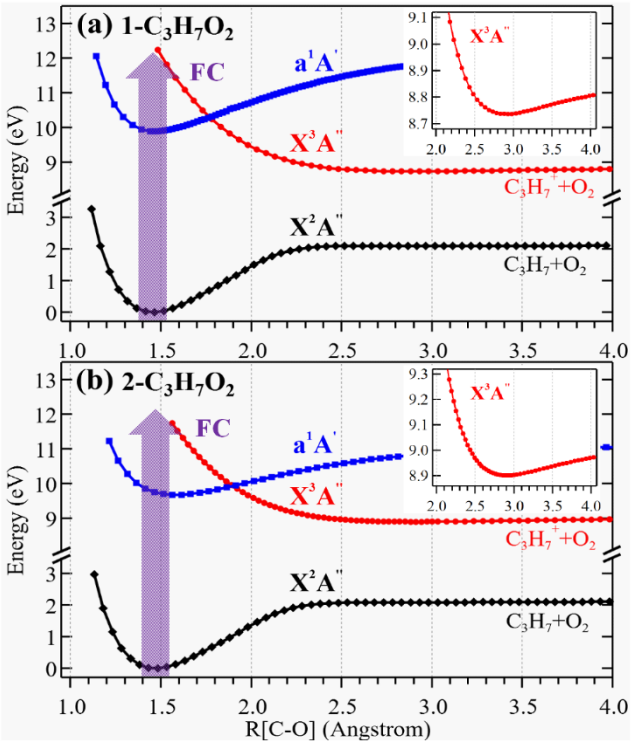

Fig. S2 Potential energy curves of (a) the G_1G_2 rotamer of 1-$C_3H_7O_2$ and (b) the G rotamer of 2-$C_3H_7O_2$, and their cations along the C-O coordinates, together with a zoom on the cationic ground state minima. The Franck-Condon (FC) region is displayed as a purple arrow.

References

1 L. Nahon, N. de Oliveira, G. A. Garcia, J. F. Gil, B. Pilette, *et al.*, *J. Synchrotron Rad.*, 2012, **19**, 508.

2 G. A. Garcia, B. K. C. de Miranda, M. Tia, S. Daly and L. Nahon, *Rev. Sci. Instrum.*, 2013, **84**, 053112.

3 G. A. Garcia, X. Tang, J.-F. Gil, L. Nahon, M. Ward, *et al.*, *J. Chem. Phys.*, 2015, **142**, 164201.

4 X. Tang, X. Gu, X. Lin, W. Zhang, G. A. Garcia, *et al.*, *J. Chem. Phys.*, 2020, **152**, 104301.

5 X. Tang, G. A. Garcia, J. F. Gil and L. Nahon, *Rev. Sci. Instrum.*, 2015, **86**, 123108.

6 G. A. Garcia, L. Nahon and I. Powis, *Rev. Sci. Instrum.*, 2004, **75**, 4989.

7 M. J. Frisch, G. W. Trucks, H. B. Schlegel, G. E. Scuseria, M. A. Robb, *et al.*, *Gaussian 09, Revision A02. Gaussian, Inc., Wallingford CT, 2016*.

8 Q. Ma and H.-J. Werner, *Wiley Interdis. Rev.: Comput. Mol. Sci.*, 2018, **8**, e1371.

9 H.-J. Werner and P. J. Knowles, *MOLPRO version 2015*, MOLPRO version 2015, http://www.molpro.net.

10 M. Hochlaf, *Phys. Chem. Chem. Phys.*, 2017, **19**, 21236.

11 M. Hochlaf, *Physics of Life Reviews*, 2020, **32**, 101.

12 H. Y. Zhao, K.-C. Lau, G. A. Garcia, L. Nahon, S. Carniato, *et al.*, *Phys. Chem. Chem. Phys.*, 2018, **20**, 20756.

13 I. Derbali, H. R. Hrodmarsson, Z. Gouid, M. Schwell, M.-C. Gazeau, *et al.*, *Phys. Chem. Chem. Phys.*, 2019, **21**, 14053.

14 G. Tarczay, S. J. Zalyubovsky and T. A. Miller, *Chem. Phys. Lett.*, 2005, **406**, 81.